

Dynamics of Air Bearing Sliders Flying on Partially Planarized Bit Patterned Media in Hard Disk Drives

Liping Li and David B. Bogy

Computer Mechanics Laboratory

Department of Mechanical Engineering

University of California

Berkeley, CA 94720

Abstract

Bit Patterned Media (BPM) recording is one of the promising techniques for future disk drives in order to increase the areal density above 1 Tbit/in². However the BPM can change the topography of the disk surface and thus have an effect on the flying characteristics of the air bearing sliders. So achieving a stable flying attitude at the Hard Disk Interface (HDI) becomes one of the main considerations for BPM. In this paper, we apply three methods (complete Homogenization, Taylor expansion Homogenization and Averaging) to solve this BPM problem and finally choose the Taylor expansion Homogenization method to investigate the slider's flying attitude on partially planarized patterned media as well as at transitions over different pattern types such as might occur at boundaries between data and servo sections.

Keywords: Bit Patterned Media, Homogenization, Averaging, Taylor Expansion, Transition, Flying height

Introduction

The hard disk drive industry is continuously trying to achieve higher data storage densities and higher reliability. Currently, achieving areal densities of 4 Tbit/in² by early 2013 and 10 Tbit/in² by the end of 2015 has become the next goal [1]. However, continuously increasing the areal density faces the challenge of thermal stability of recorded data. The proposal of BPM disks is one of the promising methods to overcome this problem since in patterned media an individual recorded bit is stored in distinct magnetic islands which are uniformly distributed on the disk.

For 1 Tbit/in² density, the pattern wavelength is estimated to be 25 nm with a feature size of 18 nm [2]. These sizes are much smaller than the air bearing slider's dimension. Several numerical techniques had been proposed to solve the slider's flying attitude on surfaces with regularly spaced surface features. Mitsuya et al. [3] introduced an Averaging method to simulate hydrodynamic lubrication of surfaces with two dimensional isotropic or anisotropic roughnesses. Later Mitsuya et al. [4] derived a simplified averaged Reynolds equation involving flow factors resulting from Boltzmann molecular free flow and applied this method to the moving roughness. Jai et al. [5] used a Homogenization method based on a double-scale approach to solve the hard disk problem with a rough slider and a rough disk. Later the Homogenization method was extended to the transient Reynolds equation derived in [6].

A number of researchers have worked on the flying characteristics of the air bearing slider (ABS) over a BPM disk. Gupta et al. [7] applied the Homogenization method to simulate the static problem of the hard disk interface (HDI) with a BPM disk without considering the effect of intermolecular forces, which occurs at sub 5nm spacing. The

relationship between the flying height, pitch, roll, stiffness and bit pattern parameters were investigated in this paper. Li et al. [8] investigated the flying characteristics of femto sliders ($0.85\text{mm}\times 0.7\text{mm}\times 0.23\text{mm}$) over BPM using direct simulation. This paper showed that a mesh size to bit diameter ratio smaller than 1:6 required to guarantee a sufficiently high resolution of the air bearing pressure. To reduce the numerical complexity of the direct method, Murthy et al. [9] transferred the pattern from the disk surface to the slider surface and limited the region of the pattern to the center trailing pad of the slider. All the above researches showed the effect of the pattern height and pattern area ratio on the slider's flying height. However, they were all analyzed for steady conditions. Knigge et al. [10] performed experiments on a disk with a flat zone and a patterned zone. They found similar results for the relationship between the flying height change and the pattern parameters. Nevertheless, because of the technical challenge of the BPM manufacture, experimental work is very limited.

Here we first apply three methods: the complete Homogenization, the Taylor expansion Homogenization method and the Averaging method to investigate the slider's dynamic flying attitude over a BPM disk. After comparing the computation times and accuracy, it is found that the Taylor expansion Homogenization method is preferable to the other two. Then this method is used to investigate the slider's flying attitude on partially planarized patterned media and at transitions over different pattern types.

Model Techniques

The BPM is modeled as uniformly distributed cylinders on a flat disk as show in Fig.1 with the bit pattern parameters shown in Fig.2, in which h is the pattern height, p is the wavelength and d is the diameter. So the area of one bit island is $\pi d^2/4$.

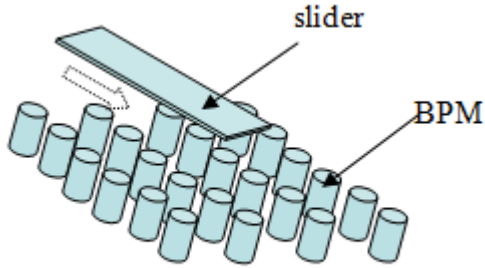


Fig. 1 Model of BPM

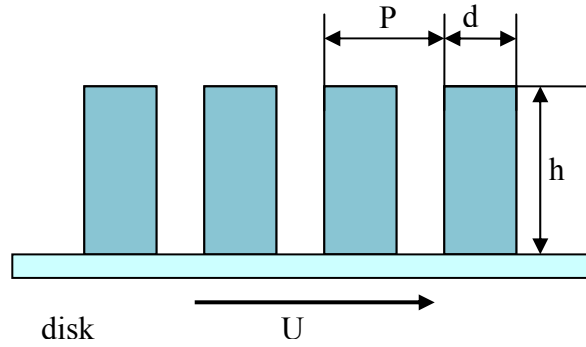


Fig. 2 Parameters of BPM

The governing equation for the gas lubricated bearing between a slider and a disk is the generalized Reynolds equation, which can be written in two space dimensions as

$$\nabla \cdot (QPH^3 \nabla P) - \nabla \cdot (HP \underline{\Lambda}) = \sigma \frac{\partial (PH)}{\partial T} \quad (1)$$

Where Q is the Poiseuille flow factor using the F-K correction [11,12]. P and H are the dimensionless pressure and spacing. $\underline{\Lambda}$ is the bearing number vector and σ is the squeeze number. T is the dimensionless time.

We assume the steady head disk spacing on an unpatterned disk is $H_0(\underline{X}, T)$ and introduce two rapid variables $\underline{y} = \frac{\underline{X}}{\varepsilon}$ and $\tau = \frac{T}{\varepsilon}$, where ε is the pattern wavelength non-dimensionalized by the slider's length. Then the spacing can be rewritten as:

$$H(\underline{X}, T, \underline{y}, \tau) = H_0(\underline{X}, T) - H^D(\underline{y} - \tau \underline{e}_U), \quad (2)$$

where H^D is an elevation of the disk surface from a reference surface. \underline{e}_U is the unit vector in the disk velocity (\underline{U}) direction. The introduction of the rapid variables requires a mesh size substantially smaller than the pattern feature size to solve Eqn. (1) directly. Obviously it is very time consuming for the computation. Since the Homogenization and Averaging methods are used to solve the roughness problem and the BPM can be thought as one kind of uniform roughness, we first turn to these two methods to solve the BPM problem.

The Homogenization method introduced in [6] includes a global problem and a local problem. The global problem is very similar to the generalized Reynolds equation except that it involves two homogenization coefficient matrixes. The local problem is a set of partial differential equations used to calculate those coefficients. The global problem is expressed as follows:

$$\nabla_x \cdot [\underline{\underline{A}}^* \nabla_x P_0] - \nabla_x (P_0 \underline{\underline{\Theta}}^*) = \sigma \frac{\partial (P_0 \bar{H})}{\partial T} \quad (3)$$

where the homogenization coefficients are:

$$\underline{\underline{A}}^* = \begin{pmatrix} \overline{QPH^3 \left(1 + \frac{\partial \omega_1}{\partial y_1}\right)} & \overline{QPH^3 \frac{\partial \omega_2}{\partial y_1}} \\ \overline{QPH^3 \frac{\partial \omega_1}{\partial y_2}} & \overline{QPH^3 \left(1 + \frac{\partial \omega_2}{\partial y_2}\right)} \end{pmatrix} \quad (4)$$

$$\underline{\underline{\Theta}}^* = \begin{pmatrix} \overline{\Lambda_x (\bar{H} + QPH^3 \frac{\partial \chi_1}{\partial y_1}) + \Lambda_y QPH^3 \frac{\partial \chi_2}{\partial y_1}} \\ \overline{\Lambda_x QPH^3 \frac{\partial \chi_1}{\partial y_2} + \Lambda_y (\bar{H} + QPH^3 \frac{\partial \chi_2}{\partial y_2})} \end{pmatrix} \quad (5)$$

Here the two over bars imply averaging with respect to the rapid variables \underline{y} and τ and over bar is the average with respect to \underline{y} . The functions $\omega_1, \omega_2, \chi_1$ and χ_2 are 1-period solutions of the following local problems:

$$-\nabla_{\underline{y}} \cdot (QP_0 H^3 \nabla_{\underline{y}} \omega_i) = \nabla_{\underline{y}} \cdot (QP_0 H^3 \underline{e}_i) \quad (6)$$

$$-\nabla_{\underline{y}} \cdot (QP_0 H^3 \nabla_{\underline{y}} \chi_i) = \nabla_{\underline{y}} \cdot ((H_0 - (1 - \frac{\sigma}{\Lambda}) H^D) \underline{e}_i) \quad (7)$$

The Homogenization method can produce quite good results [13], but it is also somewhat computationally expensive, especially for the dynamic cases. Buscaglia and Jai [14] proposed a new approach to reduce its computational cost by approximating the homogenization coefficients by a Taylor series expansion. We call this method the Taylor expansion Homogenization in this paper. In this method the coefficients A^* in (4) and Θ^* in (5) are replaced by their Taylor expansions up to order $n=4$ which was shown to be sufficiently accurate. Here the variable $\alpha = (\alpha_1, \alpha_2) = (H, P)$:

$$T_{A_n^*}(\alpha) = A^*(\alpha^0) + \sum_{i=1}^n \frac{1}{i!} ((\alpha_1 - \alpha_1^0) \frac{\partial}{\partial \alpha_1} + (\alpha_2 - \alpha_2^0) \frac{\partial}{\partial \alpha_2})^i A^*(\alpha^0) \quad (8)$$

$$T_{\Theta_n^*}(\alpha) = \Theta^*(\alpha^0) + \sum_{i=1}^n \frac{1}{i!} ((\alpha_1 - \alpha_1^0) \frac{\partial}{\partial \alpha_1} + (\alpha_2 - \alpha_2^0) \frac{\partial}{\partial \alpha_2})^i \Theta^*(\alpha^0) \quad (9)$$

The complete Homogenization method needs to solve the local problems at every node while the Taylor expansion Homogenization method only needs to solve one set or several sets of local problems. The homogenization coefficients at the other nodes can be approximated by the Taylor expansion around the coefficients which have already been calculated by solving the local problem directly.

Another method which can reduce the computational cost significantly is the Averaging method. For a moving disk, the averaged Reynolds equation is obtained as follows:

$$\nabla \cdot (QPH^3_{(ave)} \nabla P - \Lambda PH_{(ave)}) = \sigma \frac{\partial \overline{PH}}{\partial T} \quad (10)$$

where

$$H^3_{(ave)} = \alpha_p \overline{H^3} + (1 - \alpha_p) \overline{\overline{H^3}} \quad (11)$$

$$H_{(ave)} = \alpha_s \overline{H} + (1 - \alpha_s) \overline{\overline{H}} + 2\beta(1 - \alpha_s)(\overline{H} - \overline{\overline{H}}) \quad (12)$$

where \overline{H} is the arithmetic average spacing defined as $\overline{H} = \frac{\iint HdXdY}{dXdY}$ and $\overline{\overline{H}}$ is the

harmonic average spacing which is calculated by: $\overline{\overline{H}} = \overline{H^{-2}} / \overline{H^{-3}}$ and $\overline{\overline{H^3}} = 1 / \overline{H^{-3}}$. α_p

and α_s are mixing ratios given in a table in [3]. They are equal to 1 for a longitudinal pattern and equal to 0 for a transverse pattern. $\beta=1$ is for the moving disk, and $\beta=0$ is for the static disk.

The femto-sized sliders used in this study are shown in Fig. 3. The minimum flying height (MFH₀) of slider I flying over an unpatterned disk is about 2 nm while it is about 11.5 nm for slider II. In the next section we will first investigate the sliders' flying heights using the above three methods to determine the most economical method, and then we will choose this method to study the slider's attitude with a BPM disk.

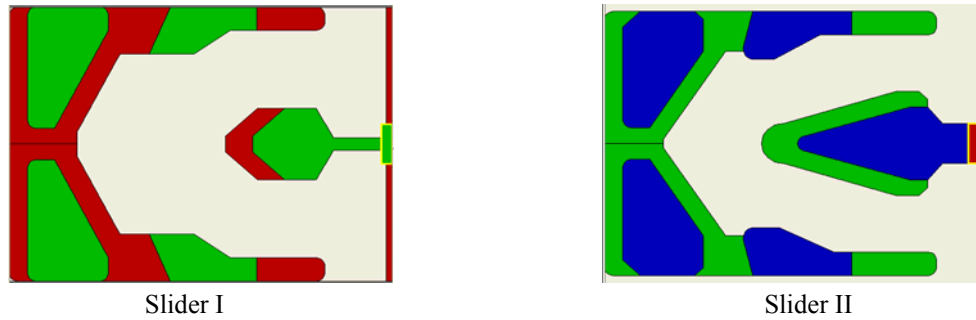


Fig. 3 parameters of BPM

Simulation results and analysis

Slider flying attitude over a BPM disk

Fig. 4 shows a comparison of the minimum flying height measured from the pattern media top surface using three methods for slider II: Averaging, Taylor expansion Homogenization and complete Homogenization method. In the figure, the abscissa shows the BPM area ratio, which is the area covered by the bit pattern divided by the total area, and PH represents bit pattern height non-dimensionalized by MFH_0 . Here the complete Homogenization method is taken as the reference method since it produces results very close to the direct simulation method [13]. The results show that for small bit pattern heights ($PH=0.1, 0.25$), both the Averaging and Taylor expansion Homogenization methods give essentially the same change tendency in the minimum flying height to bit pattern area ratio and bit pattern height: the minimum flying height increases with an increase of bit pattern area ratio and decreases with an increase of the bit pattern height. It can be explained thusly: when the bit pattern area ratio increases, the disk is covered more by the raised bit pattern so the pressure rises and the bearing force becomes larger than the suspension load. In order to balance the suspension load, the spacing should increase simultaneously. On the other hand, when the bit pattern height increases while

bit pattern area ratio keeps the same, if the slider's minimum flying height is MFH0 from the top of the patterned disk, the spacing between the slider and the disk's recess parts will increase, therefore the pressure will decrease at these parts. This leads to the spacing between the slider and the pattern's top surface decrease in order to regain the balance. These results are very similar to what was obtained in [7] for the static cases. However, as the pattern heights increase these two methods begin to produce some differences. In order to determine which method is more accurate, the slider's attitudes on two higher pattern heights (0.5, 0.75) are computed again using the complete Homogenization method. We find that the minimum flying height calculated by the Taylor expansion Homogenization method is almost the same as that from the complete Homogenization method. Moreover, the computation time of the Taylor expansion Homogenization method is almost on the same order as the Averaging method and both of them are much faster than the complete Homogenization method. So we conclude that for smaller pattern heights (pattern heights less than a quarter of the minimum flying height) we can use either the Averaging or Taylor expansion Homogenization method, but for higher pattern heights it is better to use the Taylor expansion Homogenization method. In the following study, the Taylor expansion Homogenization method is used.

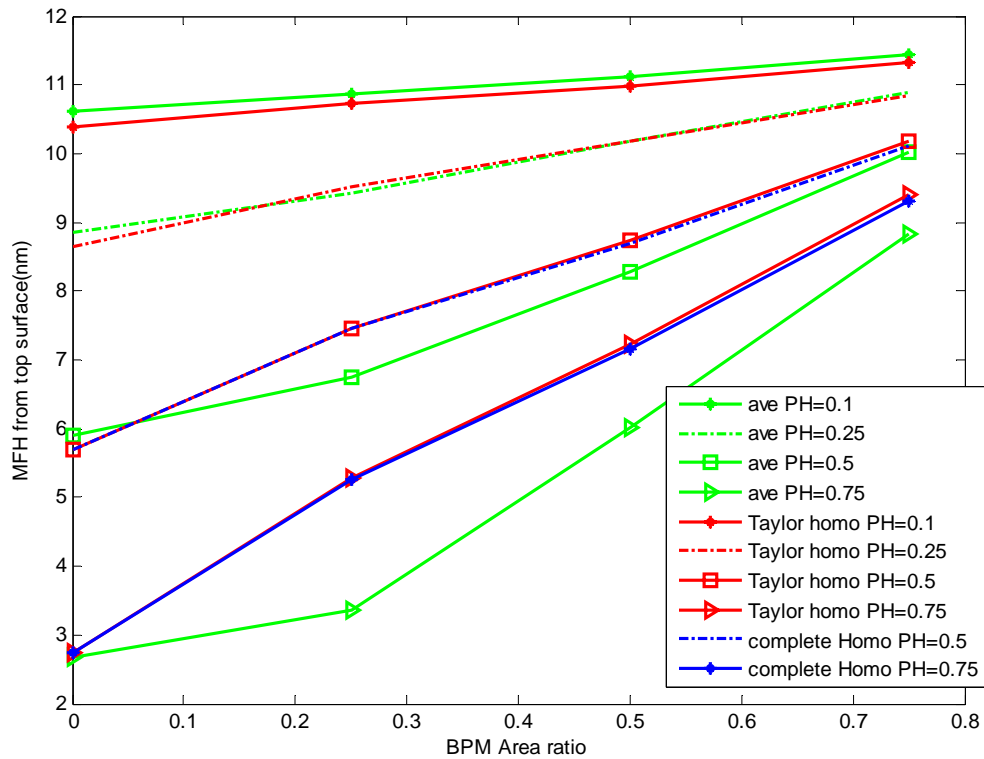


Fig.4 Comparison of minimum flying height from top surface of the pattern media using three methods

First the experiment empirical equation of the flying height loss as a function of the bit pattern height and recess area ratio in the static solutions are verified (the static solutions give almost the same results as the dynamics solutions, but much faster). Fig. 5 shows the flying height loss with a change of the bit pattern height for different recess area ratios, the number beside the line is the slope of that line. It shows the flying height loss is linearly proportional to the bit pattern height for every recess ratio. And the slope of each line is close to, but not exactly the same as, the recess area ratio represented by that line. From Fig.6 some nonlinearity is observed, especially for higher pattern height. This nonlinear effect was also obtained by the direct simulation [9] and it was explained as: a change of the bit pattern diameter leads to a change of the pattern profile not only in

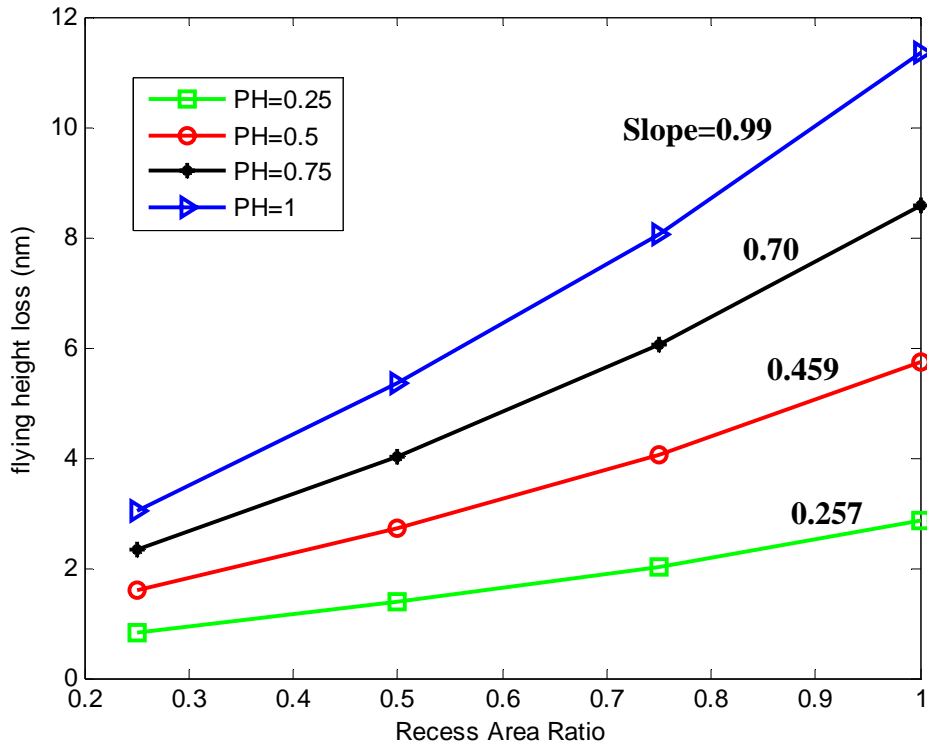


Fig.5 Flying height loss with bit pattern height for different recess area ratios

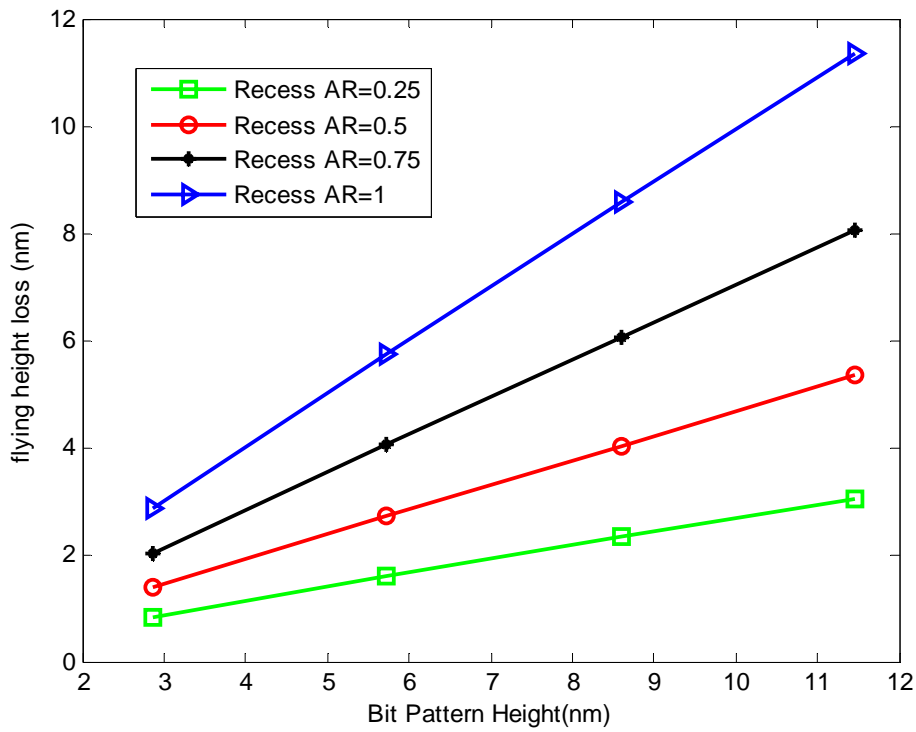


Fig.6 Flying height loss with recess area ratio for different bit pattern heights

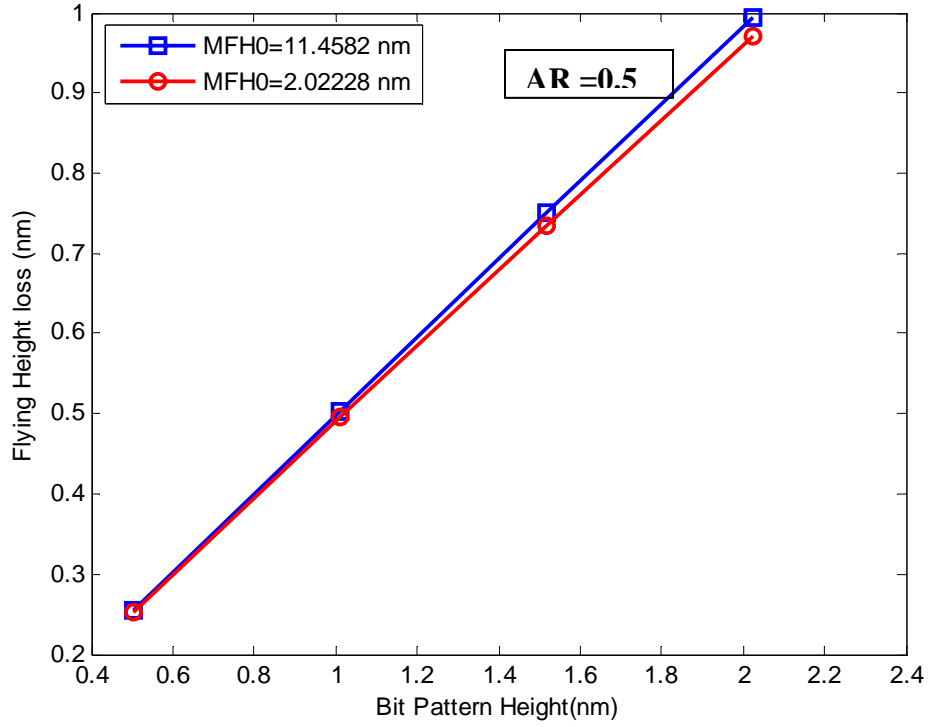


Fig.7 Flying height loss with bit pattern height for slider I and slider II

the slider's width direction but also the slider's length direction so that the side flow is prevalent in this case. However, for small pattern height, the flying height change can still be considered as a linear function of the recess area ratio. Moreover, the relationship between the flying height loss and the dimensional bit pattern height is almost independent of slider's design, which is shown in Fig.7. Thus we conclude that for small bit pattern height (such as for a more planarized bit pattern media) the empirical relationship proposed by Knigge et al. [10] is still reliable:

$$\Delta FH = h \cdot \frac{A_{recess}}{A_{total}} \quad (13)$$

Here h is the dimensional pattern height (see Fig.2), and $A_{recess}/A_{total} = 1 - \pi d^2 / p^2 / 4$.

But for high pattern heights, especially higher than MFH_0 , the above relation is not so accurate. We should simulate more cases to obtain a quadratic curve if needed.

Transition between different BPM types (different flying heights)

Next we investigate the slider's dynamic flying attitude at transitions over different pattern types, as might be associated with data and servo zones. Fig. 8 is a schematic of a slider flying at the transition between data zone and servo zone. We assume the circumferential wedge of each servo zone is about 2 degrees. So the servo circumferential length is about 1.1 mm at the computed radius and the femto slider's length is 0.85 mm.

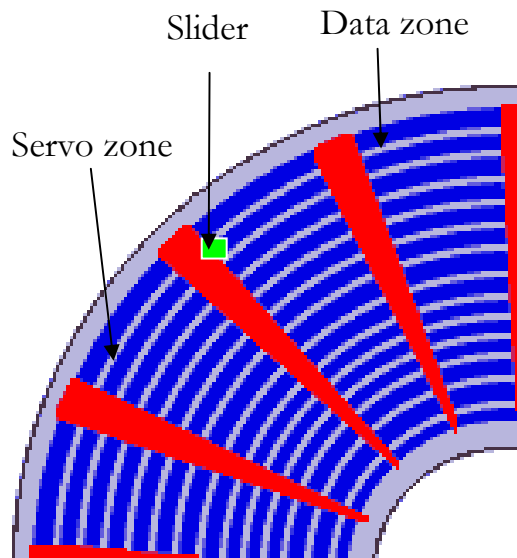


Fig.8 A slider flying at transition between data zone and servo zone

Fig. 9 shows the minimum flying height change when the slider experiences a transition between two different pattern types. Here we assume the first pattern type ($PH=0.25, AR=0.25$) covers 10 times more area than the second pattern type ($PH=0.25, AR=0.5$). From the figure, we see that the minimum flying height increases and decreases periodically during the transitions. And the minimum flying height on the

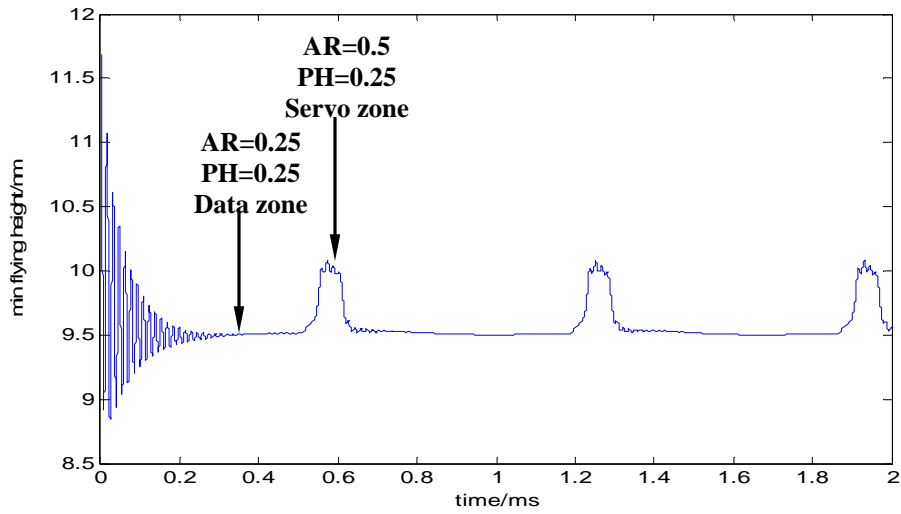


Fig. 9 Minimum flying height when the slider transition between different pattern types (same pattern height but different area ratio)

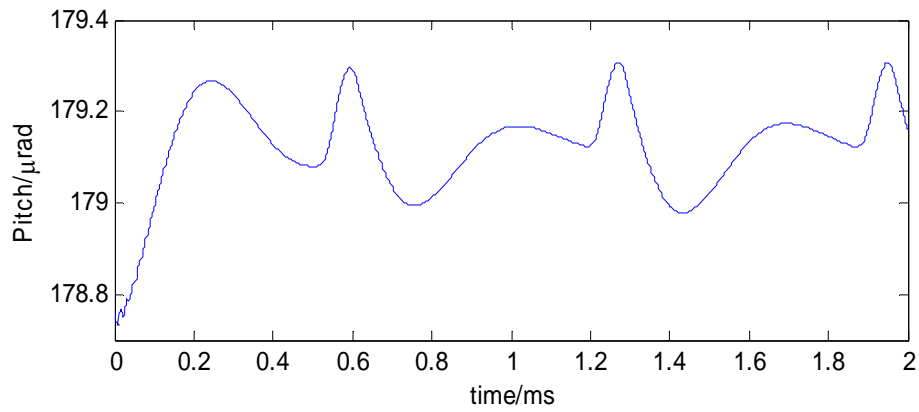


Fig.10 The pitch change when the slider transition between different pattern types

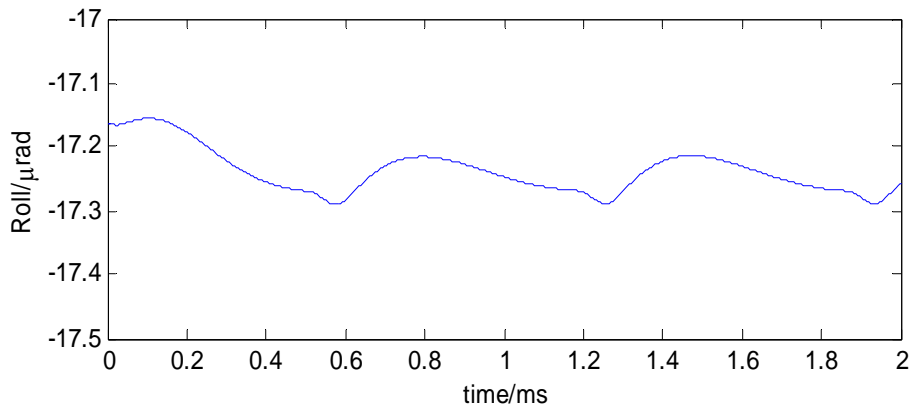


Fig.11 The roll change when the slider transition between different pattern types

first bit pattern (data zone) is almost the same as the flying height obtained in Fig. 4 for the same bit pattern type. But the minimum flying height on the second bit pattern (servo zone) has a small difference from the flying height obtained in Fig. 4. That's because the circumferential length of the second bit pattern is not long enough for the slider to obtain a steady condition. At the time the slider begins to fly from the first bit pattern to the second, one part of the slider is on the first bit pattern and the other part is on the second bit pattern. This is the reason that the slider has a gradual change during the transition. After the slider has completely transformed to the second bit pattern, it begins to seek a new steady attitude. From Fig. 10 and 11, we see the pitch and roll also change periodically when the slider experiences a transition between different pattern types. The peak-peak value of pitch is around $0.3 \mu\text{rad}$. The change of roll is even small; the peak-peak value is less than about $0.1 \mu\text{rad}$. So we can ignore the transition effect on the pitch and roll.

We also investigated the slider's flying attitude on a patterned disk with a smaller servo zone with the circumferential wedge of 0.2 degrees, which is much closer to the real disk's servo zone. In this simulation the slider first flies on the first pattern type (data zone) until it attains a steady condition and then it begins to experience transitions as shown in Fig.12. The slider's periodic motion can also be observed for this case. During transitions, the minimum flying heights on both pattern types oscillate because the circumferential length on each zone is not long enough for the slider to obtain a steady flying height. The average minimum flying height on the data zone is very close to the minimum flying height in the previous static calculation, but the flying height at the servo zone is much smaller than the previous one. When the slider flies from the data zone to

the servo zone, the flying height increases since these two zones have the same pattern height but the area ratio is larger in the servo zone than it is in the data zone. Before the slider totally transitions to the servo zone, the slider's leading edge begins to transfer to the data zone again because the circumferential length of the servo zone is smaller than the slider's length. Therefore the minimum flying height starts to decrease after a small increase (see servo zone part in Fig.12). And the peak-peak value is less than 0.25 nm which is much smaller than in the previous case. If in a real disk the circumferential wedge of the servo zone is smaller than 0.2 degrees, which is used in this simulation case, the peak-peak value will be even smaller.

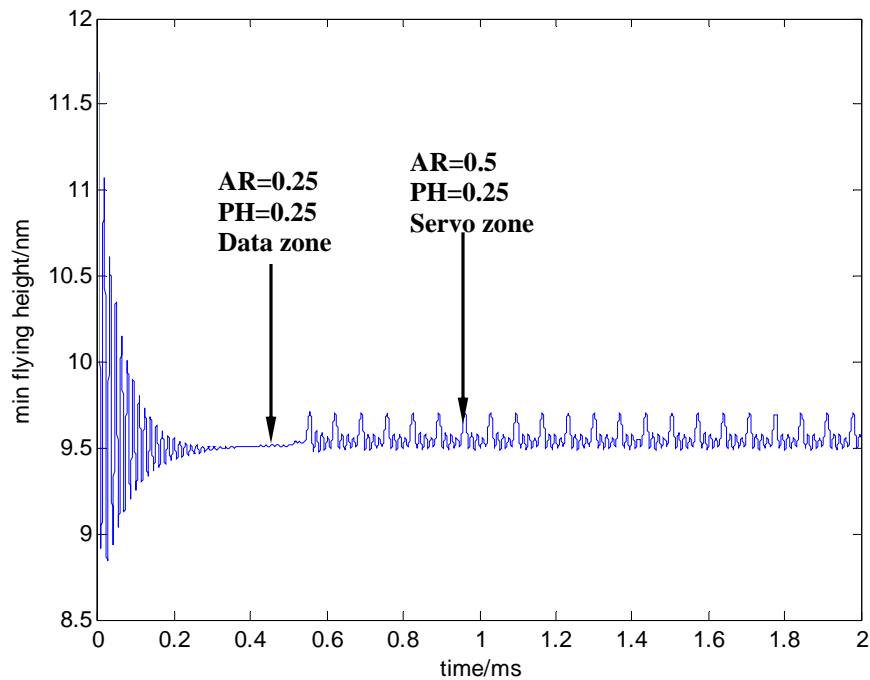


Fig.12 Minimum flying height when the slider transition between different pattern types (smaller servo zone)

Transition between different BPM types that produce a constant flying height

Here we investigate the slider's flying attitude at transitions over different pattern types which can produce the same minimum flying height. Fig.13 shows the slider's minimum flying height using the Taylor expansion Homogenization method. The horizontal straight line is used to find two different pattern types which can produce the same minimum flying height. We choose the minimum flying height of 7.5 nm for which the corresponding pattern types are: AR=0.25, PH=0.5 and AR=0.52, PH=0.75. Here we also choose the circumferential wedge of the servo zone to be 0.2 degrees. Fig.14 shows the minimum flying height change when the slider experiences a transition between the selected two pattern types. As before, the slider flies on the first pattern type until a steady state is reached and then it experiences the transitions. It turns out that the slider's flying attitude has almost no change after the slider obtains a steady condition on the first pattern type (see Figs.14-16). And this is also to be expected in actual hard disk drives.

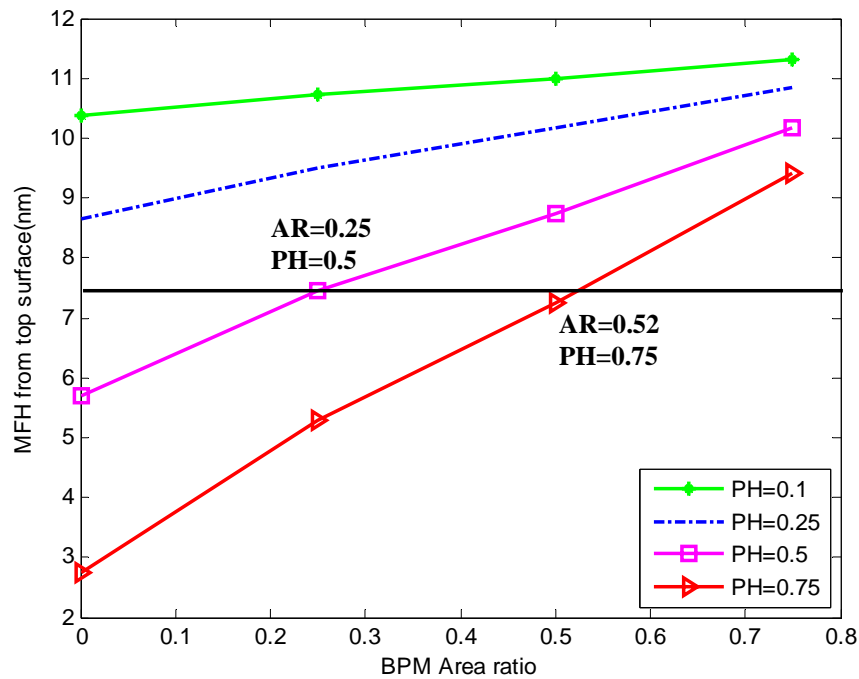


Fig.13 Two pattern types which can produce the same minimum flying height

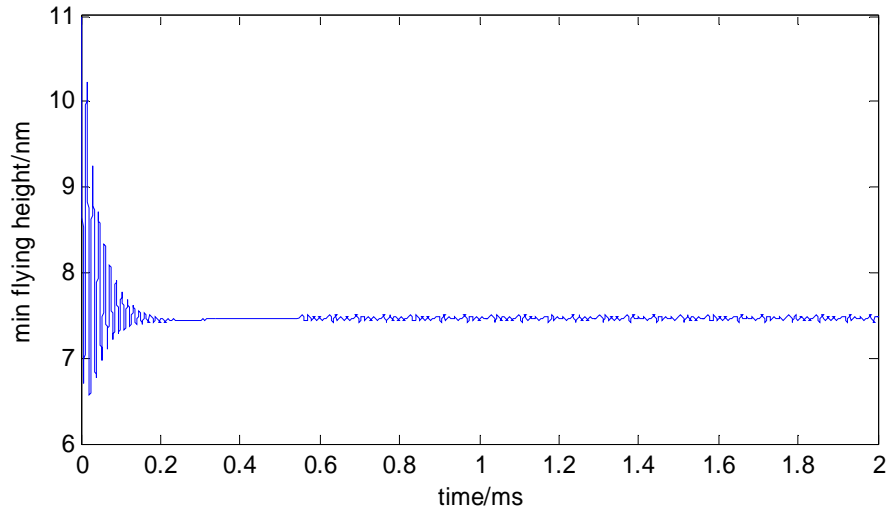


Fig.14 Minimum flying height when the slider transition between two pattern types which can produce the same minimum flying height

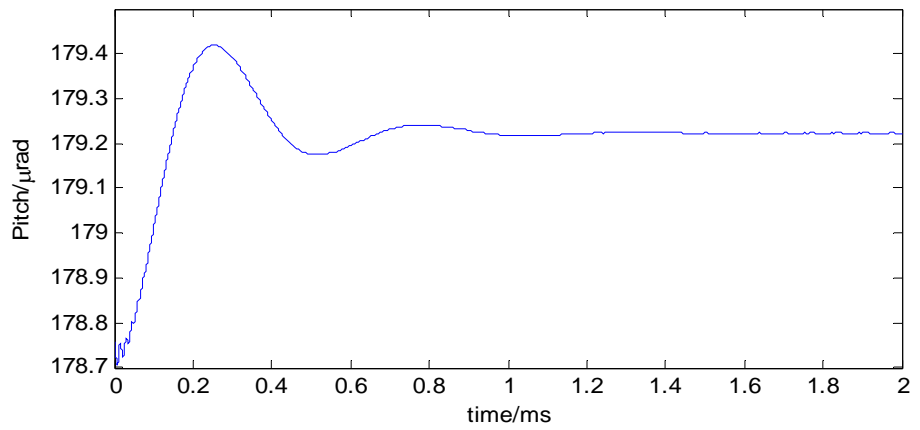


Fig.15 The pitch change when the slider transition between different pattern types

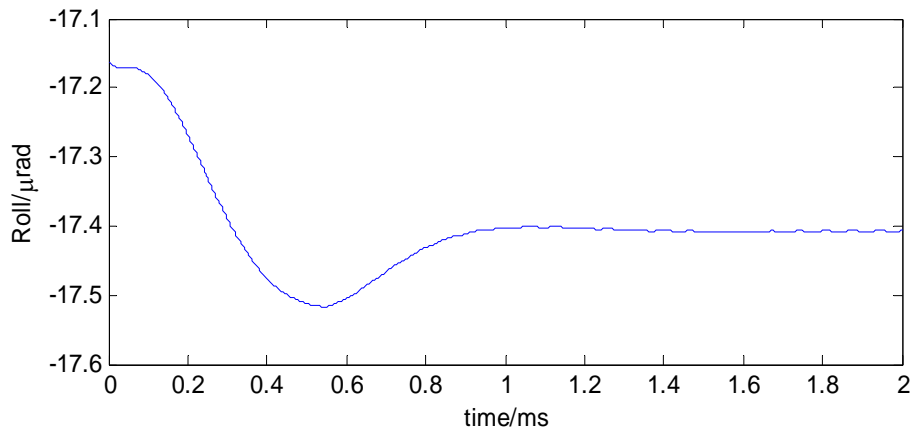


Fig.16 The roll change when the slider transition between different pattern types

Conclusion

In this paper we investigate three modeling techniques to simulate the time-dependent HDI problem for BPM disks. It is found that the Taylor expansion Homogenization is the most economical accurate method for all ranges of pattern heights while the Averaging method is only reliable for small pattern heights.

Then the Taylor expansion Homogenization method is applied to investigate the slider's flying attitude on the BPM disk. For small pattern heights, the minimum flying height loss is almost a linear function of the pattern height and area ratio. The experimentally observed empirical relation in [10] is verified. For larger pattern heights, we need to consider nonlinearities.

Next, the slider's transition between two different pattern types is also studied for both large and small circumferential wedges of the servo zone. It is found that the slider's spacing increases and decreases periodically during transitions. The pitch and roll also change periodically but the maximum change is very small. Moreover, the peak-peak value of the minimum flying height for the small servo zone is smaller than that for the larger servo zone. And for real disk this peak-peak value might be even smaller if the extent of the servo zone is smaller.

Finally, we select two different pattern types which can produce the same minimum flying height for the slider's transition study. It shows that using the selected pattern types, the slider's flying attitude remains almost constant across the transitions.

References

1. Information Storage Industry Consortium, EHDR Program. http://www.insic.org/programs_EHDR.html, December 2009.
2. Brandic Z.Z., Dobisz E.A., Wu T.W. and Albrecht T.R., 2006, "Patterned Magnetic Media: Impact of Nanoscale - Patterning on Hard Disk Drives", *Solid State Technology*, S7 Suppl. S.
3. Mitsuya Y., 1984, "A Simulation Method for Hydrodynamic Lubrication of Surfaces with Two-Dimensional Isotropic or Anisotropic Roughness Using Mixed Average Film Thickness", *Bulletin of JSME*, 27(231):2036-2044.
4. Mitsuya Y. and Koumura T., 1995, "Transient-Response Solution Applying ADI Scheme to Boltzmann Flow-Modified Reynolds-Equation Averaged with Respect to Surface-Roughness", *ASME J. Tribol*, 117(3), pg. 430-436.
5. Jai M., 1995, "Homogenization and 2-Scale Convergence of the Compressible Reynolds Lubrication Equation Modeling the Flying Characteristics of a Rough Magnetic Head Over a Rough Rigid-Disk Surface", *Mathematical Modeling and Numerical Analysis*, 29 (2), pg 199-233.
6. Buscaglia G., Ciuperca I. and Jai M., 2002, "Homogenization of the Transient Reynolds Equation", *Asymptotic Analysis*, 32(2):131-152.
7. Gupta V., 2007, "Air Bearing Slider Dynamics and Stability in Hard Disk Drives", *Ph.D. Dissertation*, Department of Mechanical Engineering, University of California – Berkeley.

8. Li H., Zheng H., Yoon Y. and Talke F. E., 2009, "Air Bearing Simulation for Bit Patterned Media", *Tribol. Lett.*, 33:199-204.
9. Murthy A., Duwensee M. and Talke F. E., 2010, "Numerical Simulation of the Head /Disk Interface for Patterned Media", *Tribol. Lett.*, 38:47-55.
10. Knigge B. E., Bandic Z.Z., Kercher D., 2008, "Flying Characteristics on Discrete Track and Bit-Patterned Media With a Thermal Protrusion Slider", *IEEE Trans. Magn.*, 44: 3656-3662.
11. Fukui S. and Kaneko R., 1988, "Analysis of Ultra-Thin Gas Film Lubrication Based on Linearized Boltzmann-Equation: First Report-Derivation of a Generalized Lubrication Equation Including Thermal Creep Flow", *ASME J. Tribol*, 110(2): 253-262.
12. Fukui S. and Kaneko R., 1990, "A Database for Interpolation of Poiseuille Flow-Rates for High Knudsen Number Lubrication Problems", *ASME J. Tribol*, 112(1):78-83.
13. Jai M. and Bou-Saïd B., 2002, 'A comparison of Homogenization and Averaging Technique for the Treatment of Roughness in Slip-Flow-Modified Reynolds Equation', *ASME J. Tribol*, 124:327-335.
14. Buscaglia G. and Jai M., 2000, "Sensitivity Analysis and Taylor Expansions in Numerical Homogenization Problems", *Numer. Math.*, 85: 49-75.